THE JOURNAL OF BIOLOGICAL CHEMISTRY
Vol. 280, No. 11, Issue of March 18, pp. 10759–10765, 2005
Printed in U.S.A.

Atomic Force Microscopy Imaging Demonstrates that $P2X_2$ Receptors Are Trimers but That $P2X_6$ Receptor Subunits Do Not Oligomerize*

Received for publication, October 29, 2004, and in revised form, January 6, 2005
Published, JBC Papers in Press, January 18, 2005, DOI 10.1074/jbc.M412265200

Nelson P. Barrera, Susan J. Ormond, Robert M. Henderson, Ruth D. Murrell-Lagnado, and J. Michael Edwardson‡

From the Department of Pharmacology, University of Cambridge, Tennis Court Road, Cambridge CB2 1PD, United Kingdom

P2X receptors are cation-selective channels activated by extracellular ATP. The architecture of these receptors is still not completely clear. Here we have addressed this issue by both chemical cross-linking and direct imaging of individual receptors by atomic force microscopy (AFM). Cross-linking of the $P2X_2$ receptor produced higher order adducts, consistent with the presence of trimers. The mean molecular volume of the receptor determined by AFM (409 nm^3) also points to a trimeric structure. $P2X_2$ receptors bearing His_6 epitope tags were incubated with anti-His_6 antibodies, and the resultant complexes were imaged by AFM. For receptors with two bound antibodies, the mean angle between the antibodies was 123°, again indicating that the receptor is a trimer. In contrast, cross-linking of the $P2X_6$ receptor did not produce higher order adducts, and the mean molecular volume of the receptor was 145 nm^3. We conclude that $P2X_2$ receptors are trimers, whereas the $P2X_6$ receptor subunits do not form stable oligomers.

P2X receptors contain an integral cation-selective ion channel that is opened by the binding of extracellular ATP (1, 2). Seven P2X receptor subunits have been identified, and these subunits associate together to form homo- or hetero-oligomeric receptors. Each subunit has two transmembrane regions (TMRs),[1] which are integrated into the membrane so that both N and C termini are intracellular. The large extracellular domain is glycosylated and contains several cysteine residues that form multiple disulfide bonds.

The architecture of P2X receptors is still not clear, although the available evidence favors a trimeric arrangement of subunits, at least for some forms of the receptor. Early indications that the receptors were oligomers arose from electrophysiological studies of both endogenous receptors and exogenously expressed receptors, which revealed that receptor activation had a Hill coefficient greater than 1 (3, 4). Analysis of the mechanism of blockade of the T336C mutant $P2X_2$ receptor by methanethiosulfonate indicated a trimeric architecture (5). More recently, chemical cross-linking of $P2X_1$, $P2X_2$, and $P2X_3$ receptors again pointed to the existence of trimers (6, 7). It is fair to say, however, that this issue has not been completely resolved. For instance, under some circumstances, the $P2X_1$, $P2X_2$, and $P2X_3$ receptors have been found to migrate on non-denaturing gels as hexamers and even nonamers (6, 7). Further, the extracellular domain of the $P2X_2$ receptor behaves as a stable tetramer in solution (8). Finally, the $P2X_6$ receptor migrates as a tetramer on native gels (7).

In the present study, we have combined a chemical cross-linking approach with direct imaging of $P2X_2$ and $P2X_6$ receptors by AFM. The ability to visualize single receptors afforded by AFM has permitted the measurement of the molecular volume of the receptors and the determination of the geometry of receptors liganded by antibodies against epitope tags present on the receptor subunits. Our data show convincingly that the $P2X_2$ receptor is a trimer, whereas the $P2X_6$ subunit is not able to form stable oligomers.

EXPERIMENTAL PROCEDURES

Cell Culture and Transient Transfection—tsA 201 cells (a subclone of human embryonic kidney (HEK) 293 cells stably expressing the SV40 large T-antigen) and normal rat kidney (NRK) cells were maintained in Dulbecco's modified Eagle's medium, containing 10% (v/v) fetal bovine serum, 2 mM glutamine, 100 units/ml penicillin, and 100 μg/ml streptomycin (Sigma), at 37 °C and in an atmosphere of 5% CO_2. cDNA encoding the rat $P2X_2$ receptor was subcloned into the pcDNA3.1/His vector (Invitrogen), which produces a protein tagged at its N terminus with the His_6 epitope. cDNA encoding the rat $P2X_6$ receptor, bearing either a hemagglutinin (HA) or a His_6 tag at its C terminus, was subcloned into the pEGFP vector, modified to remove the enhanced green fluorescent protein tag (Clontech). Transient transfections of tsA 201 cells with either $P2X_2$ or $P2X_6$ receptor DNA were carried out using the CalPhos™ mammalian transfection kit (Clontech), according to the manufacturer's instructions. Transfections of NRK cells were carried out using Lipofectamine™ (Invitrogen), again according to the manufacturer's instructions. For transfection of one 162-cm^2 culture flask, 30 μg of plasmid DNA was used. For smaller numbers of cells, amounts of DNA were scaled down appropriately. After transfection, cells were incubated for 24–48 h at 37 °C to allow expression of the P2X receptors.

Receptor Cross-linking in Crude Detergent Extracts of Transfected Cells—Transfected NRK cells, growing in 6-well plates, were washed twice with phosphate-buffered saline (150 mM NaCl, 10 mM sodium phosphate, pH 7.4) and collected directly into lysis buffer (phosphate-buffered saline, containing 1% Triton X-100 and a protease inhibitor mixture (Roche Applied Science)). The cell lysate was sonicated and then left on ice for 30 min. Samples were cleared by centrifugation at 21,000 × *g* for 15 min at 4 °C and incubated either with or without disuccinimidyl suberate (DSS; Pierce & Warriner; 4 mM) for 30 min at room temperature. Reactions were quenched by the addition of Tris-HCl, pH 7.5 (final concentration 50 mM; 15 min at room temperature) and terminated by the addition of SDS-PAGE sample buffer. In some experiments, the denatured $P2X_6$ receptor was deglycosylated by incu-

* This work was supported by Grant B19797 from the Biotechnology and Biological Sciences Research Council (to J. M. E. and R. M. H.). The costs of publication of this article were defrayed in part by the payment of page charges. This article must therefore be hereby marked "*advertisement*" in accordance with 18 U.S.C. Section 1734 solely to indicate this fact.

‡ To whom correspondence should be addressed. Tel.: 44-1223-334014; Fax: 44-1223-334040; E-mail: jme1000@cam.ac.uk.

[1] The abbreviations used are: TMR, transmembrane region; AFM, atomic force microscopy; DSS, disuccinimidyl suberate; ER, endoplasmic reticulum; GABA, γ-aminobutyric acid; HEK, human embryonic kidney; HA, hemagglutinin; NRK, normal rat kidney; CHAPS, 3-[(3-cholamidopropyl)dimethylammonio]-1-propanesulfonic acid.

bation of the cell extract with *N*-glycanase F (Roche Applied Science) for 1 h at 37 °C. Again, reactions were terminated by the addition of SDS-PAGE sample buffer. Proteins were analyzed by SDS-PAGE and immunoblotting. The $P2X_2$ receptor was detected using a rabbit polyclonal anti-receptor antibody (Alomone Laboratories; 1:500); the $P2X_6$ receptor (tagged at its C terminus with the HA epitope) was detected using a mouse monoclonal anti-HA antibody (Covance Research Products; 1:500). Immunoreactive bands were visualized using appropriate horseradish peroxidase-conjugated secondary antibodies (Perbio or Bio-Rad) followed by enhanced chemiluminescence.

Solubilization and Purification of His_6-tagged P2X Receptors—All procedures were carried out at 4 °C and are similar to those described previously for the isolation of the γ-aminobutyric acid, type A ($GABA_A$) receptor (9). Control or transfected tsA 201 cells from five 162-cm^2 culture flasks were washed twice with 10 ml/flask of HEPES-buffered saline (100 mM NaCl, 50 mM HEPES, pH 7.6), containing 2 mM EDTA. Afterward, HEPES-buffered saline, containing protease inhibitor mixture, was added to the cells, and the cells were scraped from the flasks. Each flask was rinsed with a further 10 ml of the same buffer. The combined suspension was centrifuged at 500 × *g* for 5 min at 4 °C. The supernatant was removed, and the pellet was resuspended in 6 ml of lysis buffer (10 mM Tris-HCl, pH 7.6, 2 mM EDTA, containing protease inhibitor mixture). The cells were lysed for 20 min before homogenization with a tight-fitting Dounce homogenizer. The homogenate was centrifuged at 500 × *g* for 5 min, and the resulting supernatant was again centrifuged at 21,000 × *g* for 15 min. The pellet was resuspended in solubilization buffer (100 mM HEPES, pH 7.6, 0.5 M NaCl, 1% (w/v) CHAPS, containing protease inhibitor mixture) at a protein concentration of 0.5–1.0 mg/ml. The suspension was agitated at 4 °C for 1 h and then centrifuged at 100,000 × *g* at 4 °C for 1 h to pellet unsolubilized material. Ni^{2+}-agarose binding beads (1 ml of 50% slurry; Probond, Invitrogen) were equilibrated by washing three times with 10 ml of wash buffer (HEPES-buffered saline, 0.5% (w/v) CHAPS, 10 mM imidazole). Solubilized protein was added and incubated with the beads at 4 °C for 30 min. The beads were collected by centrifugation at 300 × *g* for 3 min and then washed three times with wash buffer. The beads were packed into a small column (Invitrogen), and protein was eluted with increasing concentrations of imidazole: 2 × 200 mM and 2 × 400 mM in wash buffer (0.5-ml fractions).

Samples were analyzed by SDS-PAGE, and protein was detected by immunoblotting. The $P2X_2$ receptor was detected using either a mouse monoclonal antibody against the N-terminal His_6 tag (Invitrogen; 1:500) or a rabbit polyclonal anti-receptor antibody (see above); a mouse monoclonal anti-Myc antibody (Roche Applied Science; 1:500) was used as a negative control. The $P2X_6$ receptor was detected using a mouse monoclonal antibody against the C-terminal His_6 tag (Invitrogen; 1:500). It was found that the majority of the receptor protein was eluted in the second 200 mM imidazole fraction.

AFM Imaging of P2X Receptors and Receptor-Antibody Complexes—$P2X_2$ receptors with an N-terminal His_6 tag on each subunit were incubated either alone or following incubation with a 1:1 molar ratio (~0.2 nM each) of mouse monoclonal anti-His_6 IgG (Research Diagnostics Inc.) for 14 h at 4 °C. $P2X_6$ receptors were imaged without incubation with antibodies. Proteins were diluted in wash buffer (above) to a final concentration of ~0.04 nM, and 45 μl of the sample was allowed to adsorb to freshly cleaved, poly-L-lysine-coated mica (Sigma). After a 10-min incubation, the sample was washed with MilliQ-water and dried under nitrogen. Imaging was performed with a Multimode atomic force microscope (Digital Instruments). Samples were imaged in air, using tapping mode with a root-mean-square amplitude of 0.7 V and a drive frequency of ~300 kHz. Silicon cantilevers with a specified spring constant of 40 Newtons/meter (Mikromasch) were used.

The molecular volumes of the protein particles were determined from particle dimensions obtained from AFM images. The heights and radii were measured, usually from two cross-sections of the same particle at 90°, and the molecular volume was calculated using the following equation

$$V_m = (\pi h/6)(3r^2 + h^2) \quad \text{(Eq. 1)}$$

where h is the particle height and r is the radius at the base (10). The equation treats the protein molecules as spherical caps.

Molecular volume based on molecular mass was calculated using the equation

$$V_c = (M_0/N_0)(V_1 + dV_2) \quad \text{(Eq. 2)}$$

where M_0 is the molecular mass, N_0 is Avogadro's number, V_1 and V_2 are the partial specific volumes of particle and water, respectively, and d is the extent of protein hydration. Because the receptors are glycoproteins, the volume contributions of core protein and attached oligosaccharides were calculated separately, using previously reported values of partial specific volumes for protein (0.74 cm^3/g) and carbohydrate (0.61 cm^3/g; Ref. 11). It has been shown (10) that there are no significant differences in molecular volumes determined by imaging under fluid and in air (as in this study). Thus, for the extent of protein hydration, we used the value of 0.4 g of water/g of protein reported for a typical globular protein (human serum albumin) in solution (12).

When receptors were imaged after incubation with anti-His_6 antibodies, note was taken of whether the receptors were untagged or tagged with one, two, or three antibodies. The results obtained were expressed as a percentage of the total number of particles for each sample. Zoomed images of receptors with two antibodies bound were inspected, and the angle separating the two antibodies was measured. The distribution of angles was analyzed, and the sample mean was calculated. All errors quoted are S.E.

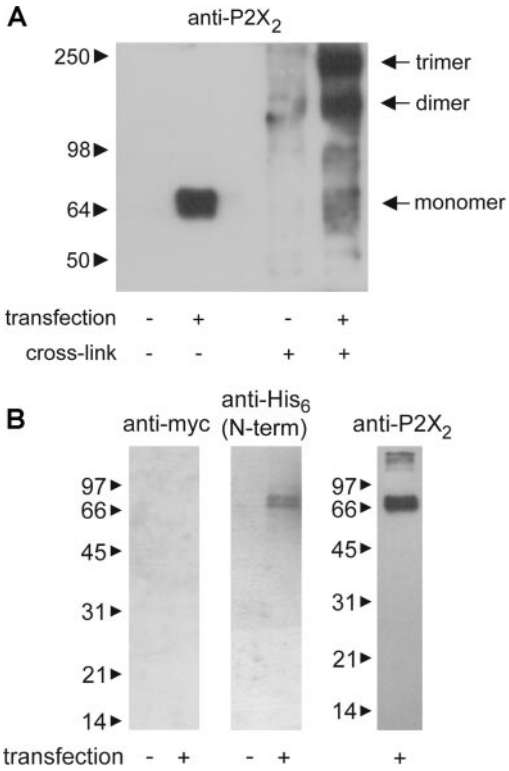

FIG. 1. **Immunoblot analysis of $P2X_2$ receptors.** *A*, cross-linking of receptors in crude detergent extracts of NRK cells. Extracts of transfected and untransfected cells were incubated either with or without the cross-linking reagent DSS (4 mM). Samples were analyzed by SDS-PAGE and immunoblotting, using a rabbit polyclonal anti-receptor antibody. Bands corresponding to subunit monomers, dimers, and trimers are indicated on the *right*. The positions of molecular mass markers (kDa) are shown on the *left*. *B*, the detection of the $P2X_2$ receptor in an eluate from a Ni^{2+}-agarose column. A band of approximate molecular mass 70 kDa is detected using both a mouse monoclonal antibody against the N-terminal (*N-term*) His_6 tag and a rabbit polyclonal anti-$P2X_2$ receptor antibody but not using a mouse monoclonal anti-Myc antibody.

RESULTS

The subunit stoichiometry of the $P2X_2$ receptor was first investigated by treating crude detergent extracts of transfected NRK cells with the cross-linker DSS. As shown in Fig. 1*A*, untransfected NRK cells did not express the $P2X_2$ receptor, whereas transfection led to robust receptor expression. The receptor migrated on SDS-polyacrylamide gels as a single band of molecular mass 70 kDa, as reported previously (7, 13, 14). When extracts of transfected cells were incubated with DSS, the 70-kDa band became much less prominent, and two new bands, of approximate molecular masses 140 and 210 kDa, appeared. This result is in agreement with a previous report (7)

and indicates that the cross-linker is revealing the presence of dimers and trimers of the receptor subunits.

To obtain more direct structural information, the $P2X_2$ receptor was isolated from transfected tsA 201 cells and analyzed by AFM. Membrane fractions of the transfected cells were solubilized in the detergent CHAPS, and the receptor was isolated through its binding to Ni^{2+}-agarose columns via its N-terminal His_6 tag. As shown in Fig. 1*B*, the isolated receptor could be detected as a 70-kDa band on blots probed with either an anti-His_6 antibody or an anti-$P2X_2$ receptor antibody. In contrast, the 70-kDa band was not detected by an antibody against the Myc epitope, which is not present in the receptor. The yield of receptor protein (~20 ng in total from a typical preparation) was too low to permit analysis of the purity of the samples by protein staining of SDS-polyacrylamide gels. Instead, sample purity was judged by AFM analysis of the protein particles, as described below.

The $P2X_2$ receptor preparation was adsorbed to a mica support, dried, and subjected to AFM imaging in air. As shown in Fig. 2, *A* and *B*, the receptor population appeared as a homogenous spread of particles. In contrast, when the standard receptor isolation procedure was applied to cells that had been mock-transfected, the resulting samples contained only 3% of the number of particles present in receptor samples, and these particles were of various sizes (data not shown). These findings indicate that the receptor samples contained very few contaminants. The heights and radii of a number of receptor particles were determined as indicated in Fig. 2, *C* and *D*. Particle radius was measured at half the maximal height to compensate for the tendency of AFM to overestimate this parameter because of the geometry of the tip (10, 15). A typical particle had a height of 2.6 nm and a radius of 9.9 nm. These values indicate a flattening of the particle, possibly caused by its drying down on the mica and/or a degree of "squashing" by the AFM tip, as observed previously (16). Particle dimensions were used to calculate molecular volumes using Equation 1. The frequency distribution of the calculated molecular volumes, based on two separate receptor preparations, is shown in Fig. 2*E*. The histogram was fitted to a Gaussian function using non-linear regression. No differences between peak and mean values were obtained ($p > 0.05$). The mean value of the molecular volume was 409 ± 18 nm^3 ($n = 91$).

As shown above (Fig. 1), the molecular mass of the $P2X_2$ receptor subunit is 70 kDa. Of this, 55 kDa is core protein, and 15 kDa is attached oligosaccharide (13). The expected molecular volume for a trimeric receptor of molecular mass 210 kDa may be estimated using Equation 2. According to this equation, the volumes of the core protein and the attached oligosaccharides should be 313 and 76 nm^3, respectively, giving a total volume of 389 nm^3.

An additional complicating factor is the likely presence of detergent bound to the TMRs of the isolated receptor. AFM imaging has been used previously to study the structure of the $GABA_A$ receptor (9), which is known to be a pentamer. When this receptor was expressed exogenously in tsA 201 cells and imaged by AFM, a mean molecular volume of 769 nm^3 was obtained. The expected value, on the basis of a total molecular mass of ~260 kDa (of which about 10% is contributed by attached oligosaccharides), is 489 nm^3. It was suggested that the considerable discrepancy between these two values was caused by the presence of detergent (9). Since each subunit of the $GABA_A$ receptor spans the membrane four times, the entire pentameric receptor would contain 20 TMRs. If the additional molecular volume (280 nm^3) were a consequence of detergent binding, this would amount to about 14 nm^3/TMR. A $P2X_2$ receptor trimer would have only six TMRs so that the expected

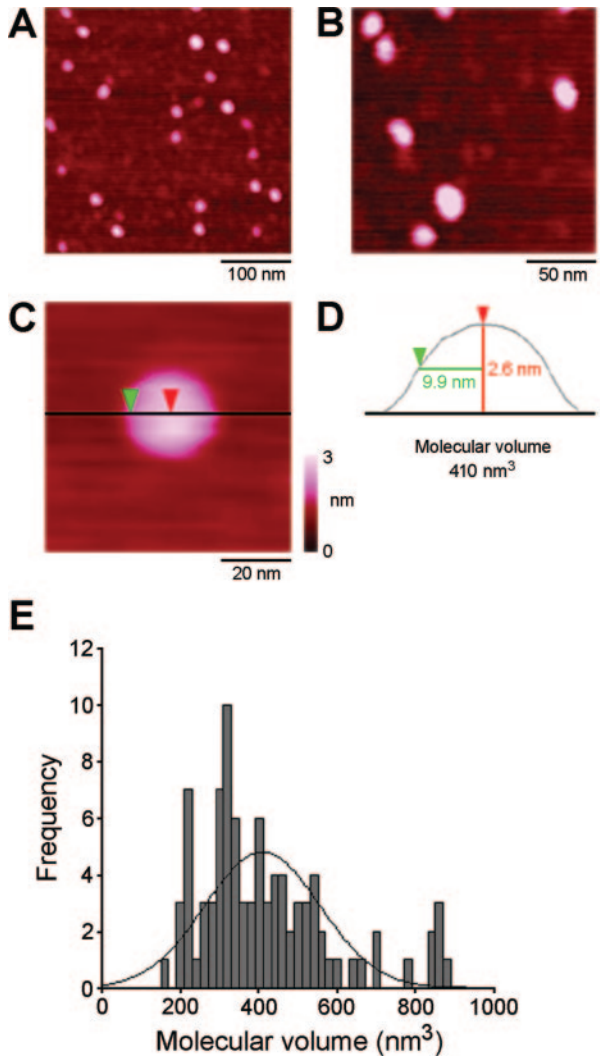

FIG. 2. **AFM imaging of $P2X_2$ receptors.** *A*, a low magnification image of $P2X_2$ receptors bound to mica. *B*, a medium magnification image of $P2X_2$ receptors. *C*, a high magnification image of a single $P2X_2$ receptor. *D*, a section through the $P2X_2$ receptor shown in *panel C*, taken at the position indicated by the *line*. The procedures for measurement of the height of the receptor (2.6 nm) and its radius at half-height (9.9 nm) are illustrated. *E*, the frequency distribution of molecular volumes of a total of 91 receptors, determined as shown in *panel D*. The curve indicates the Gaussian function that was fitted to the data. The mean (±S.E.) of the distribution is 409 ± 18 nm^3.

additional molecular volume in this case would be about 84 nm^3, which would raise the predicted total molecular volume from 389 to 473 nm^3. Given the various assumptions required to produce this value, it is clear that it should be regarded only as an estimate. Nevertheless, the molecular volume determined by AFM imaging (409 nm^3) is close to that expected of a receptor trimer (473 nm^3).

In further experiments, the receptor was imaged following incubation with a mouse monoclonal antibody that recognized the N-terminal His_6 tag. Images of the receptor alone and the antibody (IgG, molecular mass 150 kDa) alone are shown in Fig. 3*A* (*top left* and *right panels*, respectively). As can be seen, both the receptor and the antibody appeared as homogenous populations of particles, and the antibodies were clearly smaller than the receptor particles. When the suspension resulting from the receptor-antibody co-incubation was imaged, various structures were seen, including large and small particles, representing receptors and antibodies (Fig. 3*A*, *bottom panels*). Some of the large particles had one (*arrows*), two (*arrowheads*), or occasionally

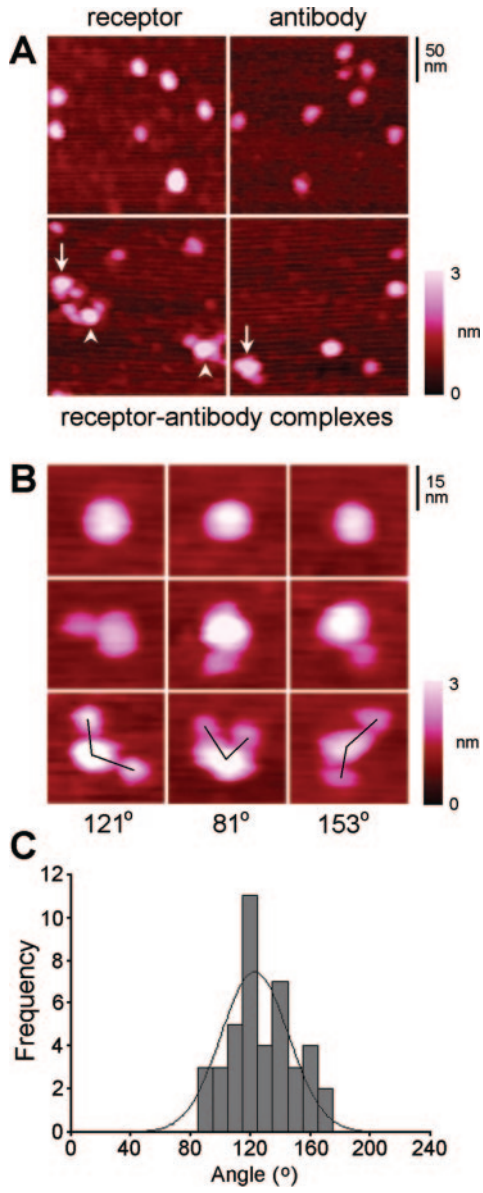

FIG. 3. **AFM imaging of complexes between $P2X_2$ receptors and anti-His_6 antibodies.** *A*, images of receptors alone (*top left panel*), anti-His_6 antibodies alone (*top right panel*), and the results of receptor-antibody co-incubation (*bottom panels*). Receptors liganded by one antibody are indicated by *arrows*; receptors liganded by two antibodies are indicated by *arrowheads*. A *color-height scale* is shown at the *bottom right*. *B*, a gallery of zoomed images of receptors that are either unliganded (*top panels*) or liganded by one (*middle panels*) or two (*bottom panels*) antibodies. The angles between the two bound antibodies in the *bottom panels* are shown. *C*, the frequency distribution of angles between antibodies for 42 doubly liganded receptors. The curve indicates the Gaussian function that was fitted to the data. The mean (±S.E.) of the distribution is 123 ± 3°.

three (not shown) smaller particles attached. These structures are likely to be receptor particles that have been liganded by one, two, or three antibody molecules. In support of this interpretation, the molecular volumes of the large particles in the various liganding states (unliganded, 411 ± 13 nm^3, n = 131; singly liganded, 396 ± 14 nm^3, n = 96; doubly liganded, 446 ± 33 nm^3, n = 42; and triply liganded, 402 ± 36 nm^3, n = 16) are all similar to each other and also to the value determined for the receptor imaged without incubation with antibody (409 ± 18 nm^3, above). The various structures in the images were analyzed, and their relative frequencies were determined. When the receptor was incubated with the anti-His_6 antibody, of 472 receptor particles analyzed, 67.4% were unliganded; 20.3% had one antibody bound, and 8.9% had two bound antibodies (Table I). A very small proportion of the receptors (3.4%) had three bound antibodies. When receptors were imaged alone, only a small percentage of the receptors (3.2% of a total of 94) appeared to be associated with bound particles. These presumably represent structures that happened to attach to the mica alongside receptors. A similar number of receptors (2.7% of a total of 301) appeared to be singly liganded following incubation with a control monoclonal antibody (anti-Myc). These data indicate that the vast majority of the binding events observed with the anti-His_6 antibody represent specific receptor-antibody interactions.

Fig. 3*B* shows a gallery of images of receptors with zero, one, and two bound antibodies. In the case of doubly liganded receptors, the angles between the pairs of bound antibodies are also shown. These angles were calculated for each complex by joining the height peaks of the antibody particles to the height peak of the receptor particle. The angles between the pairs of antibodies were determined and used to construct the frequency distribution shown in Fig. 3*C*. The mean of the distribution is 123 ± 3° (n = 42), very close to the value of 120° predicted for a trimeric receptor.

Fig. 4 summarizes our conclusions regarding the architecture of the $P2X_2$ receptor, based on the data presented above. The individual receptor subunits span the membrane twice (Refs. 1 and 2) (Fig. 4*A*). These subunits are arranged as trimers to produce the complete receptor (Fig. 4*B*). According to this receptor architecture, two antibodies against the His_6 tags added to the subunits should bind to the receptor with an angle of 120° between them. AFM images of doubly liganded receptors confirm this arrangement (Fig. 4*C*).

When the $P2X_6$ receptor is expressed exogenously in cells such as *Xenopus* oocytes or cultured olfactory bulb neurons, only a very small minority of the receptor is delivered to the cell surface (7, 17). Instead, the majority of the $P2X_6$ receptor resides in the endoplasmic reticulum (ER), suggesting that it is being retained by the "quality control" machinery of the cell. One possible reason for this retention is that the receptor is not being correctly assembled, perhaps because the $P2X_6$ receptor subunits are unable to oligomerize. To test this possibility, we first subjected crude extracts of transfected NRK cells to treatment with the cross-linker DSS. As shown in Fig. 5*A*, untreated receptor migrated on SDS-polyacrylamide gels as a major band of molecular mass 52 kDa and a minor band of molecular mass 45 kDa. These sizes are consistent with the existence of the receptor in glycosylated and unglycosylated forms (7). To confirm this interpretation, a denatured cell extract was incubated with *N*-glycanase F, which should remove all *N*-linked oligosaccharides from the receptor. As expected, this treatment caused the two receptor bands to collapse into one band of approximate molecular mass 45 kDa (Fig. 5*B*). When the cell extract was treated with DSS, the two bands corresponding to the monomeric form of the receptor remained, and no clear higher order adducts were produced (Fig. 5*C*). Instead, there was a "smear" migrating between molecular masses 80–150 kDa, suggesting that the receptor had been cross-linked to a variety of neighboring proteins.

The cross-linking data suggest that the $P2X_6$ receptor, unlike the $P2X_2$ receptor, does not form homo-trimers within the cells. To examine this possibility directly, the His_6-tagged receptor was isolated from CHAPS extracts of membrane fractions through its ability to bind to Ni^{2+}-agarose and imaged by AFM. Typical images of the isolated $P2X_6$ receptor attached to mica, at two different magnifications, are shown in Fig. 6, *A* and *C*. Images of the $P2X_2$ receptor, at these same magnifications, are also shown for purposes of comparison (Fig. 6, *B* and *D*). Simple

TABLE I
Antibody tagging profile of the $P2X_2$ receptor

Number of particles bound to receptor	Receptor alone	%	Receptor plus anti-His_6 antibody	%	Receptor plus anti-Myc antibody	%
0	91	96.8	318	67.4	292	97.0
1	3	3.2	96	20.3	8	2.7
2	0	0	42	8.9	1	0.3
3	0	0	16	3.4	0	0

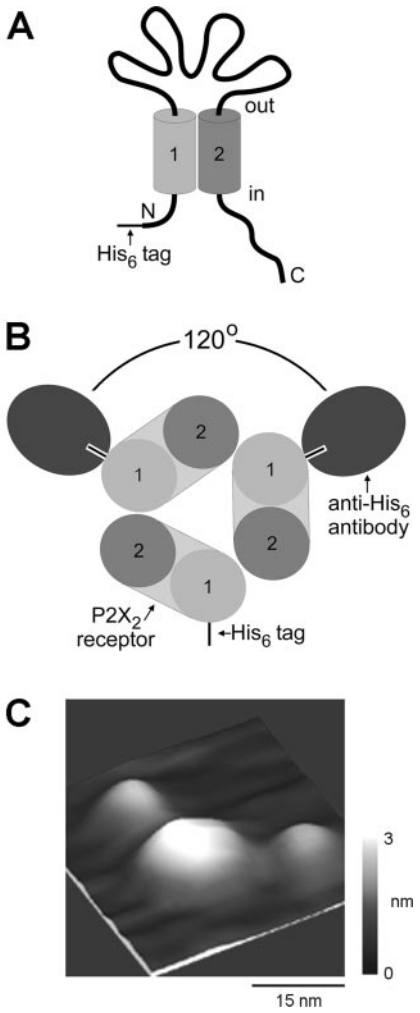

FIG. 4. **Trimeric model of $P2X_2$ receptor assembly based on the data presented.** *A*, a diagram of a single receptor subunit, indicating the two membrane-spanning domains, the long extracellular loop, and the intracellular N and C termini. The position of the His_6 tag on the N terminus is shown. *B*, the arrangement of antibodies bound to two His_6 tags, assuming a trimeric receptor architecture. *C*, a three-dimensional AFM image of a receptor liganded by two anti-His_6 antibodies. The angle between the bound antibodies is 121°, as expected from the model shown in *panel B*. A *shade-height scale* is shown at the *bottom right*.

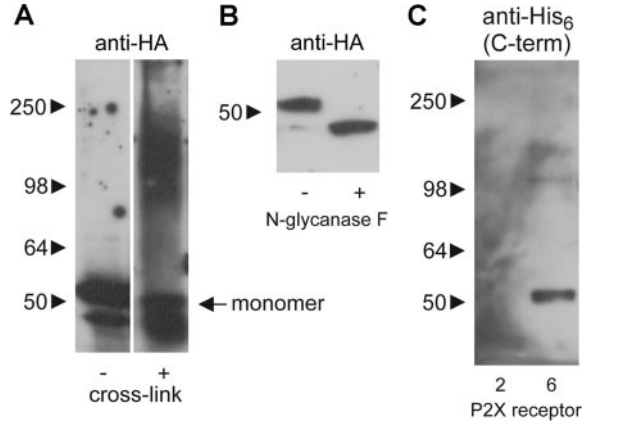

FIG. 5. **Immunoblot analysis of $P2X_6$ receptors.** *A*, the treatment of receptors in crude detergent extracts of transfected NRK cells with the cross-linking reagent DSS (4 mM). Samples were analyzed by SDS-PAGE and immunoblotting, using a mouse monoclonal antibody against the C-terminal HA epitope tag. The band corresponding to the glycosylated receptor monomer is indicated on the *right*. The positions of molecular mass markers (kDa) are shown on the *left*. Note that no clear higher order adducts are produced by treatment with DSS. *B*, the effect of treatment of the cell extract with *N*-glycanase F. Note that the doublet originally present collapses into a single band of molecular mass 45 kDa. *C*, the detection of the $P2X_6$ receptor in an eluate from a Ni^{2+}-agarose column. A band of approximate molecular mass 52 kDa is detected using a mouse monoclonal antibody against the C-terminal His_6 tag. Note that this antibody does not detect the isolated $P2X_2$ receptor, which has the His_6 tag on its N terminus.

inspection of these images reveals that the $P2X_6$ receptors are, on average, considerably smaller than the $P2X_2$ receptors. Measurement of the heights and radii enabled the calculation of the molecular volumes of the particles, using Equation 1. A typical particle had a height of 1.6 nm and a half-height radius of 7.6 nm. A frequency distribution of the calculated molecular volumes is shown in Fig. 6*E*, with the distribution for the $P2X_2$ receptor for comparison. As for the $P2X_2$ receptor, the histogram for the $P2X_6$ receptor was fitted to a Gaussian function using non-linear regression. Again, no differences between peak and mean values were obtained ($p > 0.05$). The mean of the distribution is 145 ± 7 nm^3 ($n = 117$). The predicted value for a $P2X_6$ subunit of molecular mass 52 kDa, calculated using Equation 2 and taking into account the contributions of core protein and attached oligosaccharides, is 97 nm^3. Detergent binding, to the extent of 14 nm^3/TMR (above), would increase the predicted molecular volume of a monomer to 125 nm^3, close to the measured value. These results indicate that the $P2X_6$ receptor subunits do not form stable oligomers.

DISCUSSION

The results of our chemical cross-linking experiments are consistent with those reported previously (6, 7) and strongly suggest that the membrane-associated $P2X_2$ receptor is a trimer. It is clear from previous reports, however, that this indirect method for studying receptor structure has the potential to generate confusing results. We therefore sought a more direct method for examining receptor architecture.

AFM permits the visualization of single isolated proteins and the measurement of their molecular dimensions (9, 10, 18–20). A comparison of the molecular volume of individual receptors determined in this way with the volume expected for a particular molecular mass provides information about the subunit stoichiometry of the receptor. Schneider *et al.* (10) have shown a very good correlation between predicted and calculated molecular volumes, over a range of protein molecular masses from 38 to 900 kDa. In the current study, the molecular volume of the $P2X_2$ receptor determined in this study (409 nm^3) was close to the value predicted using the assumption that the receptor is a trimer of 70-kDa subunits (473 nm^3).

There was considerable variation in the calculated molecular volume for the $P2X_2$ receptor. There are likely to be several sources of this variation. First, it is unlikely that the receptor is

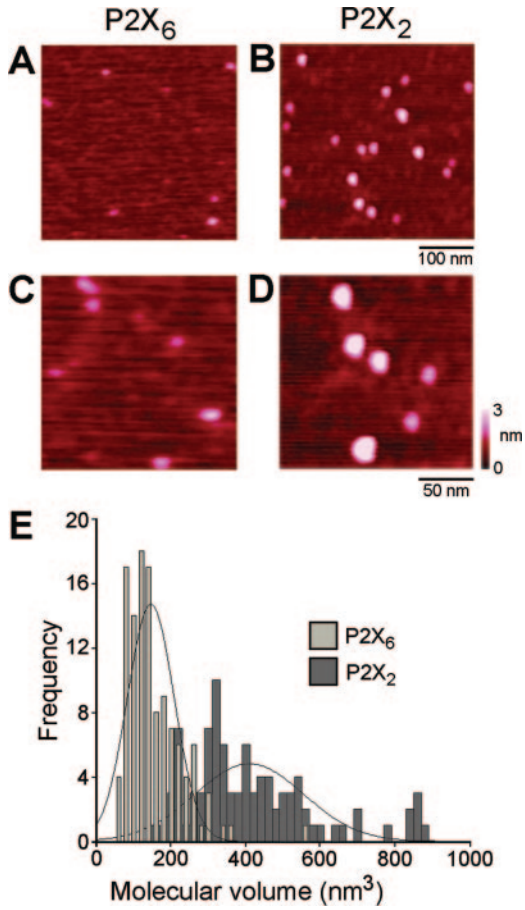

FIG. 6. **AFM imaging of isolated $P2X_6$ receptors.** *A*, a low magnification image of $P2X_6$ receptors bound to mica. *B*, an image of isolated $P2X_2$ receptors at the same magnification, for purposes of comparison. *C*, a medium magnification image of $P2X_6$ receptors. *D*, an image of $P2X_2$ receptors, at the same magnification. A *color-height scale* is shown at the *bottom right*. *E*, the frequency distributions of molecular volumes of 117 $P2X_6$ receptors and 91 $P2X_2$ receptors (taken from Fig. 2*E* for comparison). The curves indicate the Gaussian functions that were fitted to the data. The mean (± S.E.) of the distribution for the $P2X_6$ receptor is 145 ± 7 nm^3.

completely pure, and any impurities will of course have various molecular volumes. Second, the receptor will probably attach to the mica surface in a range of orientations. This will lead to aberrations in the calculation of molecular volume, which is based on the assumption that the receptor has the shape of a spherical cap. Third, there may be differences in the amount of detergent remaining attached to the various receptor particles. However, despite these sources of variation, the standard error on the calculated molecular volume (<5%) is relatively small.

For reasons described above, it is probably unwise to rely exclusively on molecular volume calculations to determine receptor architecture. Fortunately, AFM imaging provides a second means of examining receptor structure, based on antibody decoration of tags placed on individual subunits. We have applied this method previously in our study of the $GABA_A$ receptor (9). The predominant form of this receptor in the brain contains α_1-, β_2-, and γ_2-subunits (21), probably in the stoichiometry of 2α:2β:1γ (22). We set out to determine whether the two α_1-subunits known to be present within the $GABA_A$ receptor pentamer were adjacent or separated by another subunit. To address this question, we placed His_6 tags on the α_1-subunits, isolated the tagged receptor, and incubated it with anti-His_6 antibodies. When we imaged the receptor-antibody complexes bound to mica, we found a number of receptors that had been decorated with two antibodies. The mean angle between the antibodies was 135°, close to the value of 144° expected if the α-subunits were separated by another subunit, rather than the 72° expected for adjacent α-subunits (9). In the present study, we identified receptors that had been decorated with two anti-His_6 antibodies. The mean angle between the antibodies was 123°, very close to the 120° expected for a trimeric receptor. The method used relies on the receptor-antibody complexes attaching to the mica in a manner that reflects the orientation of the antibodies in solution (*i.e.* falling flat so that the receptor and the two antibodies are all resting on the mica). Further, if the attachment formed between the receptor and the antibodies has some degree of flexibility, then one would expect this to be reflected in a variation in the angles measured. As expected from these considerations, there was indeed some variation in the values of angles calculated (between 80 and 170°), which is reflected in the images shown in Fig. 3*B*. Nevertheless, the standard error of the distribution of angles was small (~2% of the mean), indicating that these problems are not significant.

When expressed in *Xenopus* oocytes, $P2X_6$ receptors fail to reach the cell surface and instead remain in the core glycosylated form, consistent with their retention in the ER (7). A similar behavior is seen in olfactory bulb neurons, where exogenously expressed $P2X_6$ receptors co-localize with the ER marker calreticulin (17). Transfected HEK 293 cells do express some $P2X_6$ receptors at their cell surface (23). These receptors are typically non-functional, although there has been a report of functional activity in a small minority of stably transfected HEK 293 cell clones (24). ER localization of receptors normally indicates incorrect assembly and retention by the ER quality control system. In the case of the cells expressing functional $P2X_6$ receptors at the cell surface, it was suggested that additional proteins might be assisting in the correct assembly of the receptors (24).

Recently, it was reported that $P2X_6$ receptor subunits expressed in *Xenopus* oocytes behave as tetramers and large aggregates on native gels (7). In contrast, it has been shown that co-expression of FLAG-tagged and HA-tagged $P2X_6$ receptor subunits in HEK 293 cells did not result in co-immunoprecipitation, unlike the results obtained for all the other P2X receptor subunits (25). This latter result suggests that all subunits except $P2X_6$ are able to form stable homo-oligomers. To directly assess the oligomerization state of $P2X_6$ receptors in tsA 201 cells, we determined the molecular volume of isolated receptors and compared it with the value expected on the basis of the subunit molecular mass. $P2X_6$ receptor subunits imaged on mica were obviously smaller than $P2X_2$ receptors, and the measured molecular volume (145 nm^3) was close to the value expected for a single subunit with bound detergent (125 nm^3). We conclude, therefore, that the $P2X_6$ receptor is unable to form stable oligomers and propose that this failure to assemble is indeed the reason why the receptor does not traffic efficiently to the cell surface in *Xenopus* oocytes or HEK 293 cells. There remains the possibility that our choice of detergent with which to solubilize the receptor (CHAPS) was inappropriate and that oligomers would have been seen if another detergent had been used. The behavior of P2X receptors has, in fact, been found previously to be detergent-dependent (6), although differentially epitope-tagged $P2X_2$ receptor subunits could be co-immunoprecipitated after solubilization in various detergents (25). Further, the fact that the $P2X_2$ receptor behaves as trimer in CHAPS indicates that this detergent is not having a deleterious effect on receptor assembly.

We have demonstrated that AFM imaging can be used successfully to provide important information about the architecture of two types of ionotropic receptor (the P2X receptor and the $GABA_A$ receptor (9)). We anticipate that further progress

can now be made using this approach. For instance, it ought to be possible to determine the subunit stoichiometry and architecture of other homomeric P2X receptors and of heteromeric P2X receptors. We also plan to apply the same techniques to study the structures of other members of the ionotropic receptor superfamily.

REFERENCES

1. Khakh, B. S. (2001) *Nat. Rev. Neurosci.* **2,** 165–174
2. North, R. A. (2002) *Physiol. Rev.* **82,** 1013–1067
3. Bean, B. P. (1990) *J. Neurosci.* **10,** 1–10
4. Ding, S., and Sachs, F. (1999) *J. Gen. Physiol.* **113,** 695–720
5. Stoop, R., Thomas, S., Rassendren, F., Kawashima, E., Buell, G., Surprenant, A., and North, A. R. (1999) *Mol. Pharmacol.* **56,** 973–981
6. Nicke, A., Bäumert, H. G., Rettinger, J., Eichele, A., Lambrecht, G., Mutschler, E., and Schmalzing, G. (1998) *EMBO J.* **17,** 3016–3028
7. Aschrafi, A., Sadtler, S., Niculescu, C., Rettinger, J., and Schmalzing, G. (2004) *J. Mol. Biol.* **342,** 333–343
8. Kim, M., Yoo, O. J., and Choe, S. (1997) *Biochem. Biophys. Res. Commun.* **240,** 618–622
9. Neish, C. S., Martin, I. L., Davies, M., Henderson, R. M., and Edwardson, J. M. (2003) *Nanotechnology* **14,** 864–872
10. Schneider, S. W., Lärmer, J., Henderson, R. M., and Oberleithner, H. (1998) *Pfluegers Arch. Eur. J. Physiol.* **435,** 362–367
11. Durchschlag, H., and Zipper, P. (1997) *J. Appl. Crystallogr.* **30,** 803–807
12. Grant, E. H. (1957) *Phys. Med. Biol.* **2,** 17–28
13. Torres, G. E., Egan, T. M., and Voigt, M. M. (1998) *FEBS Lett.* **425,** 19–23
14. Jiang, L.-H., Kim, M., Spelta, V, Bo, X., Surprenant, A., and North, R. A. (2003) *J. Neurosci.* **23,** 8903–8910
15. Lärmer, J., Schneider, S. W., Danker, T., Schwab, A., and Oberleithner, H. (1997) *Pfluegers Arch. Eur. J. Physiol.* **434,** 254–260
16. Neish, C. S., Martin, I. L., Henderson, R. M., and Edwardson, J. M. (2002) *Brit. J. Pharmacol.* **135,** 1943–1950
17. Bobanovic, L. K., Royle, S. J., and Murrell-Lagnado, R. D. (2002) *J. Neurosci.* **22,** 4814–4824
18. Ellis, D. J., Dryden, D. T. F., Berge, T., Edwardson, J. M., and Henderson, R. M. (1999) *Nat. Struct. Biol.* **6,** 15–17
19. Berge, T., Ellis, D. J., Dryden, D. T. F., Edwardson, J. M., and Henderson, R. M. (2000) *Biophys. J.* **79,** 479–484
20. Saslowsky, D. E., Lawrence, J., Ren, X., Brown, D. A., Henderson, R. M., and Edwardson, J. M. (2002) *J. Biol. Chem.* **277,** 26966–26970
21. McKernan, R. M., and Whiting, P. J. (1996) *Trends. Neurosci.* **19,** 139–143
22. Farrar, S. J., Whiting, P. J., Bonnert, T. P., and McKernan, R. M. (1999) *J. Biol. Chem.* **274,** 10100–10104
23. Chaumont, S., Jiang, L.-H., Penna, A., North, R. A., and Rassendren, F. (2004) *J. Biol. Chem.* **279,** 29628–29638
24. Jones, C. A., Vial, C., Sellers, L. A., Humphrey, P. P. A., Evans, R. J., and Chessell, I. P. (2004) *Mol. Pharmacol.* **65,** 979–985
25. Torres, G. E., Egan, T. M., and Voigt, M. M. (1999) *J. Biol. Chem.* **274,** 6653–6659